

Anomalous quantum glass of bosons in a random potential in two dimensions

Yancheng Wang,^{1,2} Wenan Guo,^{1,3,*} and Anders W. Sandvik^{4,†}

¹*Department of Physics, Beijing Normal University, Beijing 100875, China*

²*Institute of Physics, Chinese Academy of Sciences, Beijing 100190, China*

³*State Key Laboratory of Theoretical Physics, Institute of Theoretical Physics, Chinese Academy of Sciences, Beijing 100190, China*

⁴*Department of Physics, Boston University, 590 Commonwealth Avenue, Boston, Massachusetts 02215, USA*

(Dated: June 25, 2018)

We present a quantum Monte Carlo study of the “quantum glass” phase of the 2D Bose-Hubbard model with random potentials at filling $\rho = 1$. In the narrow region between the Mott and superfluid phases the compressibility has the form $\kappa \sim \exp(-b/T^\alpha) + c$ with $\alpha < 1$ and c vanishing or very small. Thus, at $T = 0$ the system is either incompressible (a Mott glass) or nearly incompressible (a Mott-glass-like anomalous Bose glass). At stronger disorder, where a glass reappears from the superfluid, we find a conventional highly compressible Bose glass. On a path connecting these states, away from the superfluid at larger Hubbard repulsion, a change of the disorder strength by only 10% changes the low-temperature compressibility by more than four orders of magnitude, lending support to two types of glass states separated by a phase transition or a sharp cross-over.

PACS numbers: 64.70.Tg, 67.85.Hj, 67.10.Fj

There are two types of ground states of interacting lattice bosons in the absence of disorder; the superfluid (SF) and the Mott-insulator (MI). In the Bose-Hubbard model (BHM) with repulsive on-site interactions [1, 2] an MI state has an integer number of particles per site and there is a gap to states with added or removed particles. The gapless SF can have any filling fraction. These phases and the quantum phase transitions between them are well understood [1–6] and have been realized experimentally with ultracold atoms in optical lattices [7, 8].

If disorder in the form of random site potentials is introduced in the BHM (which can also be accomplished in optical lattices [9, 10]) a third state appears—an insulating but gapless quantum glass. This state has been the subject of numerous studies [1–3, 11–27] but many of its properties are still not well understood. Two types of glass states are known; the compressible Bose glass (BG) and the incompressible Mott glass (MG), with the latter commonly believed to appear only at commensurate filling fractions in systems with particle-hole symmetry [18–20, 26–29]. The currently prevailing notion is that the glass state in the 2D BHM with random potentials is always of the compressible BG type [20–22, 25].

We here present quantum Monte Carlo (QMC) results for the two-dimensional (2D) site-disordered BHM, showing that there is actually an extended parameter region in which the BG is either replaced by an MG or has an anomalously small (in practice undetectable) compressibility. The system is described by the Hamiltonian

$$H = -t \sum_{\langle ij \rangle} (b_i^\dagger b_j + b_j^\dagger b_i) + \frac{U}{2} \sum_{i=1}^N n_i(n_i - 1) + \sum_{i=1}^N \epsilon_i n_i, \quad (1)$$

where $\langle ij \rangle$ are nearest neighbors on the square lattice, b_i^\dagger (b_i) are boson creation (destruction) operators, $n_i = b_i^\dagger b_i$

site occupation numbers, and ϵ_i random potentials uniformly distributed in the range $[-\Lambda - \mu, \Lambda - \mu]$ about the average chemical potential μ . We study the model using the stochastic series expansion (SSE) QMC method with directed loop updates [30]. We adjust the chemical potential so that the mean filling-fraction $\rho = \langle n_i \rangle = 1$ (to within $< 10^{-5}$) when averaged over sites i , disorder realizations, quantum and thermal fluctuations. To speed up the simulations, we impose a cut-off $n_i \leq 2$ (some times $n_i \leq 3$) which does not change the nature of the states. We study sufficiently large inverse temperatures $\beta = t/T$ and lattice sizes L ($N = L^2$ sites) to address the ground state in the thermodynamic limit.

In the plane $(\mu/U, t/U)$, for fixed disorder strength Λ , there are characteristic “Mott lobes” inside which the filling is integer, while outside ρ changes with μ, U [2, 3, 11–18, 21–25]. The lobes are surrounded by a quantum glass (Griffiths) phase for any $\Lambda > 0$ [21–25]. At fixed integer filling, in the plane (U, Λ) there is a narrow “finger” of the glass phase intervening between the MI and SF, shrinking to a point U_c at $\Lambda = 0$. Most studies have focused on $\rho = 1$ and the phase diagram in this case is qualitatively very similar in two [25] and three [22] dimensions. We show a schematic phase diagram in Fig. 1.

We focus first on a vertical line in the phase diagram in Fig. 1 at moderate U . With increasing Λ we can go from the MI, transition into the glass state in the finger region, then into the SF, and finally re-enter a glass state at much larger Λ . We also consider a line to the right of the SF phase in Fig. 1, studying the evolution of the glass with increasing disorder when the SF is not crossed but (as we will show) the properties change dramatically.

We compute two observables characterizing the states: the compressibility κ and the superfluid stiffness ρ_s (obtained with SSE using, respectively, particle-number and

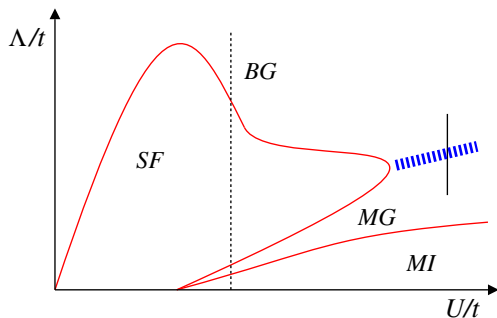


FIG. 1. (Color online) Schematic phase diagram in the plane of repulsion U and disorder strength Λ of the 2D BHM with random potentials and filling $\rho = 1$. We study the system along the dashed line spanning the Mott insulator (MI), putative Mott glass (MG), superfluid (SF), and Bose glass (BG). The boundary or cross-over between the MG and BG is indicated by the thick dashed line, and we also traverse it in calculations along a vertical (solid) line.

winding number fluctuations [30]). The results were averaged over 500 – 1000 realizations of the random potentials. Fig. 2 shows the evolution with Λ of these quantities for a fixed system size at a low temperature.

Before discussing the results, we recall the reasons for the existence of a glass phase and its expected nature. In disordered systems in general, one can expect Griffiths phases where statistically rare large regions of some phase inside another phase lead to singularities not present in the absence of disorder [31–33]. For the integer- ρ BHM with site disorder, the Griffiths argument states the following [2, 3]: Once the width 2Λ of the disorder distribution exceeds the Mott gap Δ_M , there can be arbitrarily large domains of SF inside the MI. Until Λ exceeds some larger critical value these domains are not percolating through the lattice, and the state is therefore insulating [34]. In the standard scenario (discussed further in supplementary material), fluctuations of the overall chemical potential within the SF domains lead to near degeneracies of different particle-number sectors and, therefore, nonzero compressibility (a BG) [21, 22, 25]. With these notions in mind, we now discuss our results.

Looking first at the superfluid stiffness in Fig. 2, the sharp increase at $\Lambda \approx 8$ signals the entry into the SF phase. A finite-size scaling analysis, presented below, shows that the transition takes place at $\Lambda_c \approx 8.3$, which is in reasonable agreement with the result by Söyler *et al.*, $\Lambda_c(U = 22) \approx 7.8$ [25]. Here we note that our model is slightly different, because of the cut-off $n_i \leq 2$ (while there was no cut-off in Ref. [25]). When we increase the cut-off to $n_i \leq 3$ the critical point moves to a value consistent with that of Söyler *et al.* Increasing Λ further in Fig. 2, the superfluid stiffness eventually again decreases to zero at $\Lambda \approx 30$. This transition point is much smaller than that of Söyler *et al.*, $\Lambda_c \approx 70$, as would be expected in this region where the probability of site occupations beyond our cut-off is substantial. Since the cut-off does

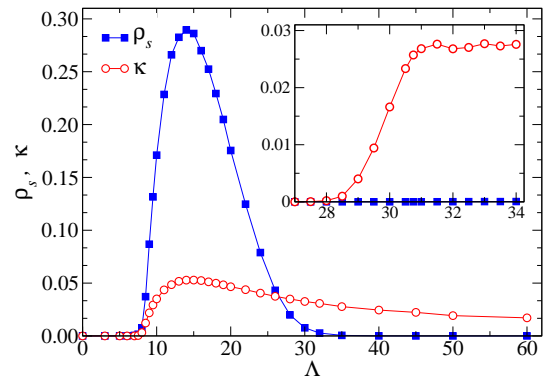


FIG. 2. (Color online) Compressibility and superfluid stiffness vs disorder strength in a 16×16 system at $\beta = 8$. At $U = 22$ (main graph), the system evolves from glass to SF and back to glass. Results for $U = 60$ are shown in the inset. Here the system stays in the glass phase but the compressibility changes rapidly around $\Lambda = 30$ (far away from the Mott boundary at $\Lambda \approx 24$).

not alter any symmetries of the system there is no reason to believe that it will affect our conclusions regarding the nature of the phases and transitions.

Turning to the compressibility, it is substantial in the SF phase and when the glass is re-entered at large Λ . However, it is very small below the SF transition, not only in the Mott phase (which extends up to $\Lambda \approx 4.3$ in our system, based on the Mott gap of the clean MI as discussed in supplementary material) but also in the region $\Lambda \approx 5 - 7$, where the system is in a glass phase. The $L \rightarrow \infty$ compressibility as a function of temperature is shown in Fig. 3. At $\Lambda = 0$ and 3, we observe the normal exponential decay with β expected in the gapped MI phase. At $\Lambda = 6$ and 7 we instead find the form

$$\kappa \sim \exp(-b/T^\alpha) + c, \quad (2)$$

where $\alpha < 1$ and $c = 0$ (to within statistical errors). This form has previously been found in random quantum spin systems [29, 35], where κ corresponds to the magnetic susceptibility and one expects it to vanish as $T \rightarrow 0$ because of spin-inversion symmetry (corresponding to particle-hole symmetry for bosons). Such an incompressible and insulating quantum glass is called an MG [13] and has also been shown to exist in variants of the 2D random BHM where particle-hole symmetry is explicitly built in [27, 28] (and Ref. [13] argued for its possible existence also more generally). To our knowledge, $\kappa(T)$ was not computed for these systems and there is no theoretical prediction for its form. In the presence of random potentials there is no explicit particle-hole symmetry (but in principle there could be emergent particle-hole symmetry, as in the clean BHM at the tips of the Mott lobes [2]). It had been argued that the glass state of the BHM should then always be a clearly compressible BG [21, 22, 25] (except very close to the MI boundary),

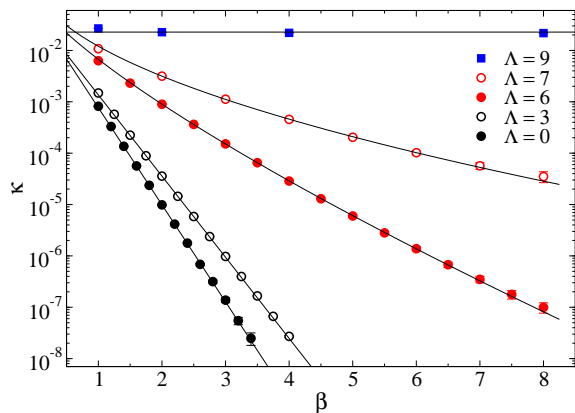


FIG. 3. (Color online) Compressibility versus inverse temperature for $U = 22$ and different strengths Λ of the disorder. The lattice size $L = 32$ in all cases, which is sufficient to eliminate finite-size effects at these temperatures. The curves are fits to the form (2) with $\alpha = 1$ for $\Lambda = 0, 3$ (MI state) and $\alpha = 0.78$ and 0.53 for $\Lambda = 6$ and 7 , respectively (MG state). For $\Lambda = 9$ (SF state) κ is essentially constant.

contrary to our findings.

While $c = 0$ in (2) may not hold strictly, the very small $\kappa(T \rightarrow 0)$ at the very least shows that the system is an anomalous BG, with exceedingly small (essentially undetectable) compressibility in a large part of the phase diagram. We here use the term MG because, as we will argue below, even if $c > 0$ but small the physics behind the anomalous BG is very similar to a true MG.

The form (2) of $\kappa(T)$ with $c = 0$ can be understood heuristically as follows: Consider non-Mott domains below the percolation point inside an MI. At temperature T there is some size m such that for $T \lesssim m^{-a}$ all domains of size $s < m$ are effectively in their ground states and do not contribute to the compressibility. The exponent a depends on the low-energy level spectrum of the domains, which should be related to the fractal nature of the domains. Domains with $s > m$ should contribute essentially independently of T and s . The probability of a site belonging to a domain of size $s > m$ is $\propto \exp(-dm^b)$, where b can in principle be computed using classical percolation theory [36] (but may be different in a quantum system). In terms of the unknown exponents a and b the compressibility due to non-Mott domains is $\kappa \propto \exp(-dT^{-b/a})$, which is Eq. (2) with $\alpha = b/a$.

The above scenario neglects the arbitrarily close degeneracy of different particle-number sectors due to fluctuations of the average chemical potential of the domains, which lead to $\kappa(T = 0) > 0$ in the standard BG scenario (where the non-Mott domains are superfluid). How can these degeneracies be avoided? By studying isolated domains with a different chemical potential embedded in an MI, we have found (see supplementary material) that there are finite-size effects due to which particle-number degeneracies in the region of interest here only

occur when the domains are large (with the critical size diverging at the Mott phase boundary). All domains below a critical size (which depends on the domain shape) have vanishing $T \rightarrow 0$ compressibility and should not be regarded as superfluid—they are insulating because of finite size and effectively possess particle-hole symmetry at low energy. One still expects rare domains exceeding the critical size to contribute when $T \rightarrow 0$. However, we will show below that typical large domains should also have an altered spectral structure due to quantum-criticality when the SF boundary is approached. Thus, both small and large typical domains (the latter of which are fractals) may not contribute to the $T = 0$ compressibility.

Within the standard scenario, there should still exist rare large compressible domains in the Mott background, but in reality the domains are never completely isolated from each other and the picture of degenerate single-domain levels may ultimately not be valid away from the atomic limit (large U and Λ). Whether or not strictly $c = 0$ in Eq. (2), in practice the compressibility is undetectably small and the system is effectively an MG in the finger region (and, as we will see, also at larger U in a substantial region along the Mott boundary).

We do find a compressible BG in the re-entrance region at large Λ (above the SF in Fig. 1), as illustrated by results at $\Lambda = 60$ in Fig. 4. There should then be a phase transition or a cross-over separating the MG and the BG phases. We have identified a dramatic variation in the compressibility along a vertical line at $U = 60$. As shown in the inset of Fig. 2, at $\beta = 8$, κ increases rapidly with Λ between 28 to 31 (which is far away from the Mott boundary at $\Lambda \approx 24$), before flattening out. The enhancement is more than four orders of magnitude, κ being very small before the sharp increase. We do not find any significant finite-size effects in this region for $L > 8$, and also the behavior does not change substantially upon further increasing β (and the n_i cut-off also does not play a role here). The behavior therefore indicates a sharp cross over, not a phase transition, though in principle κ could still vanish exponentially at some point away from the Mott boundary. As a function of U , the cross-over most likely occurs on a line extending out from the right-side SF tip (“nose”) [34] in Fig. 1 and can be interpreted as a change from a state where typical non-Mott domains are not superfluid to a BG where the domains are superfluid but do not form a coherent global state.

We next study the critical $T = 0$ compressibility at the lower glass-SF boundary, where $\kappa \sim (\Lambda - \Lambda_c)^{\nu(2-z)}$ is expected in the thermodynamic limit. If $z = 2$, as is often assumed [21, 22, 25], $\kappa > 0$ is non-singular at the transition. One would then expect $\kappa > 0$ also close to the transition inside the glass [18]. Then the only plausible scenario is that $\kappa > 0$ throughout the glass phase (and there is no *a priori* reason to expect a very small κ). A key question then is whether $z = 2$ or $z < 2$. In the former

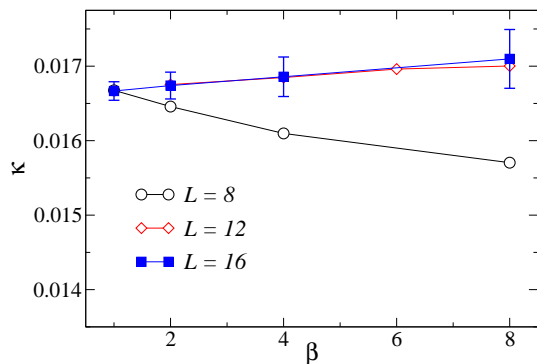


FIG. 4. (Color online) Compressibility versus inverse temperature for systems with $U = 22$, $\Lambda = 60$. Error bars are only shown for $L = 16$ (being much smaller for $L = 8, 12$).

case divergent SF clusters in the MI background close to the percolation point would be compressible, while in the latter case they should be incompressible. There are arguments for $z = 2$ at the glass-SF transition [2] but no rigorous proofs. Some numerical works on models related to the BHM have in fact pointed to $z < 2$ [37, 38]. Calculations suggesting $z = 2$ are affected by large uncertainties [11, 17, 18] and are also consistent with $z < 2$.

We extract z using the following finite-size scaling behaviors [2] expected exactly at the critical point:

$$\kappa(L, \Lambda_c) \propto L^{z-d}, \quad \rho_s(L, \Lambda_c) \propto L^{-z}. \quad (3)$$

In Fig. 5 we show results using different system sizes and scaling the inverse temperature according to $\beta = L^z$ with three choices of z [39]. Based on Eqs. (3) we expect curves of κL^{d-z} for different L to cross each other at a point (asymptotically for large L) if the correct value of z is used, and a similar behavior of $\rho_s L^z$. It should be noted, however, that there are crossings even if a wrong z is used, but the vertical crossing value (e.g., for system sizes L and $2L$) will then drift up or down instead of converging to a constant. One can also expect larger corrections to the horizontal crossing value if an incorrect z is used. The compressibility crossing points in Fig. 5 are very sensitive to the value of z , while the stiffness crossings are more stationary. Such behavior has also been observed in certain clean bosonic systems [40]. Based on our result, z should be between 1.5 and 1.75, which implies that the percolating SF cluster is incompressible.

In the above analysis it has been implicitly assumed that any non-singular contributions to κ can be neglected. If regular contributions arise from SF domains larger than a critical size, then we would expect these contributions to increase with L and, by Eq. (3), this would lead to an apparent *enhancement* of z . Since we instead find a reduction from $z = 2$ it appears that non-singular background contributions are not responsible for this effect and $z < 2$ should be a robust result. It is also interesting to note the distinct drop in compressibility in

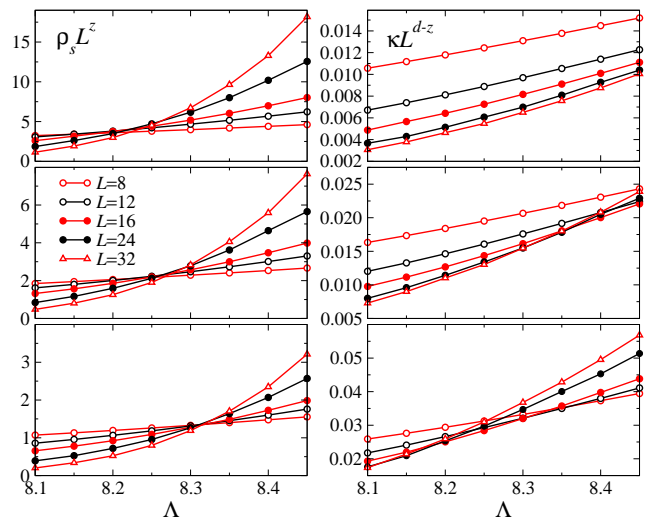


FIG. 5. (Color online) Finite-size scaling of the superfluid stiffness (left column) and the compressibility (right column) for $U/t = 22$ using three different values of the dynamic exponent; $z = 2, 1.75$, and 1.5 (top to bottom) [39].

Fig. 2 at the lower SF to glass transition, while at the second transition there are no strong variations, suggesting large regular contributions there, or, possibly, $z = 2$.

Along with a large critical size needed for non-Mott domains to become superfluid, even far away from the Mott boundary, a dynamic exponent $z < 2$ provides an explanation for an anomalously small, or possibly vanishing, $T = 0$ compressibility in the finger region of the phase diagram between the Mott and SF phases. The sharp cross-over from anomalously small to normal compressibility away from the SF phase at larger U also shows that there are two distinct types of glass phases in the BHM, one being either an MG or an anomalous BG with physics similar to an MG, and the other one a standard BG with isolated non-coherent superfluid domains.

The scenario discussed here applies only to integer filling fractions, since a compressible state follows trivially from a non-constant $\rho(U, \Lambda)$ for incommensurable systems. Differences between integer and non-integer filling were found in a recent renormalization-group study [23], although it is not clear whether the state is the MG or anomalous BG identified in our work.

Acknowledgments.—We thank Claudio Chamon, Matthew Fisher, Philip Phillips, Anatoli Polkovnikov, Nikolay Prokof'ev, and Boris Svistunov for discussions. This research was supported by the NSFC under Grant No. 11175018 (WG) and by the NSF under Grants No. DMR-1104708 and PHY-1211284 (AWS). WG would like to thank Boston University's Condensed Matter Theory Visitors program. AWS gratefully acknowledges travel support from Beijing Normal University.

SUPPLEMENTARY MATERIAL

We here describe how we have determined the Mott gap of the clean Bose-Hubbard model, using the SSE QMC method and finite-size analysis. This gap allows for an accurate determination of the Mott-glass phase boundary of the site-disordered model. We also discuss how the standard scenario of non-interacting superfluid “lakes” in the site-disordered model gives rise to a non-zero compressibility κ in the limit $T \rightarrow 0$. This scenario does not take into account finite-size effects of the lakes (among other approximations), and including those effects significantly reduce the value $\kappa(T \rightarrow 0)$. We demonstrate this by studying a single domain with altered chemical potential inside a Mott insulator. To demonstrate sufficient statistics in the calculation of the disorder-averaged compressibility κ , we also present probability distributions (histograms) of κ . They exhibit some tails in the glass phase, but not significant enough to cause sampling problems related to rare occurrences at the temperatures considered. Finally, we demonstrate the small effects of the cut-off imposed on the site occupation numbers n_i in the SSE simulations.

1. Determination of the Mott gap

It is not easy to determine the phase boundary between the Mott insulating (MI) and glass phase of the site-disordered Bose-Hubbard model (BHM) by direct studies of properties of the glass phase, because in that region its properties are completely dominated by very large and extremely rare “lakes” of the non-Mott phase (which are normally assumed to be superfluid) inside the Mott background.[3] It is, however, well known that the phase boundary is completely determined by the Mott gap Δ_M of the clean system as it is this gap that has to be overcome by the average chemical potential of a large lake for such a lake to become superfluid (see recent discussion and calculations in, e.g., Refs. 21, 22, and 25). It is easy to find the density as a function of chemical potential in a clean finite system by using QMC methods, and the Mott gap can be extracted from such curves as the width of the constant part, where the density ρ is integer. Determining the MI-glass boundary by finite-size scaling of the gaps is the most straight-forward aspect of studies of the phase diagram of the site-disordered BHM in the plane (U, Λ) of Coulomb repulsion and disorder strength.

As a prelude to discussing finite-size effects of the non-Mott lakes in Sec. 3, we here demonstrate our calculations of the Mott gap with value quoted in the main text, including effects of the cut-off n_{\max} of the site occupation numbers n_i in the SSE QMC simulations.[30]

The density versus chemical potential is shown for a 16×16 system for $n_{\max} = 2$ and 3 in the top panel of

Fig. 6. The $\rho = 1$ plateau is very clearly visible and slightly narrower for $n_{\max} = 3$ (and naturally the effects of the cut-off are larger on the right-hand side of the plateau, where the particle number fluctuates to higher values). A large number of smaller density jumps for higher and lower chemical potentials are smeared into smooth curves by finite-temperature effects, even at the relatively low temperature ($\beta = 1/T = 32$) used here. The middle and bottom panels of Fig. 6 show results at several different temperatures in the neighborhood of the left edge of the $\rho = 1$ plateau. Here the particle number, $\langle n \rangle = N\rho$, is graphed instead of ρ . Plateaus at all integer values are expected in $\langle n \rangle$ versus μ if the temperature is low enough. Here we can clearly see the step between $\langle n \rangle = 255$ and 256 developing for $\beta = 256$. The μ point at which the curves cross the half-way distance between these two particle numbers provides a convenient and well convergent (versus β) way of defining the edge of the $\rho = 1$ plateau, which then is used in combination with the analogous step on the right-side to extract the Mott gap (here for the two different cut-offs).

In Fig. 7 we show the finite-size scaling of $\Delta_M(L)$ extracted for several different system sizes at $U = 22$. Given that the system has a finite correlation length, the gap is expected to converge exponentially fast, once L exceeds this correlation length, and our results are consistent with such a form. The extrapolated Mott gap is $\Delta_M = 8.52(2)$ and $\Delta_M = 8.10(2)$ for $n_{\max} = 2$ and $n_{\max} = 3$, respectively. The latter value is very close to the value obtained in Ref. 5 without restrictions on the occupation numbers.

2. Independent superfluid lakes scenario

Consider a system of N sites. Denoting the total number of bosons by n , the compressibility is given by

$$\kappa = \frac{1}{NT} \left[\langle n^2 \rangle - \langle n \rangle^2 \right]. \quad (4)$$

For a system in the Mott phase n is an integer multiple of N with no fluctuations at $T = 0$.

Consider now a simplified model of a system with random potentials in which clusters of N_i sites form lakes with chemical potential $\mu_i = \mu + \epsilon_i$, with the disorder values ϵ_i uniformly distributed in the interval $[-\Lambda, \Lambda]$ and the lakes labeled $i = 1, \dots, N_l$. Sites that do not belong to these clusters form a Mott-insulating background with chemical potential μ at the center of the Mott gap. Assume further that the Mott background is completely “rigid”, so that the superfluid lakes can be considered completely independent of each other (i.e., the numbers n_i of particles in each lake are uncorrelated). Then the

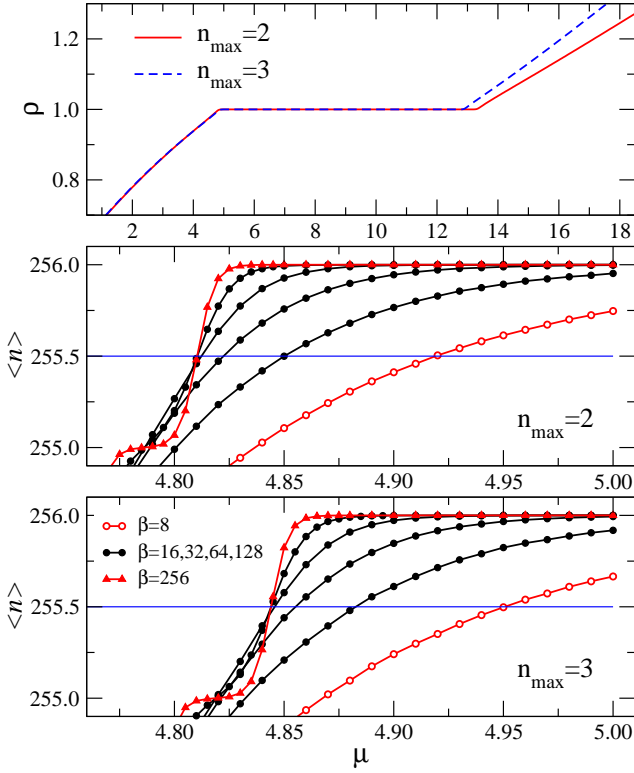


FIG. 6. (Color online) SSE QMC results for the particle density ρ and the particle number $\langle n \rangle = N\rho$ of the clean $L = 16$ BHM with $U = 22$ as a function of the chemical potential μ . Two different cut-offs, $n_{\max} = 2, 3$, were used. The top panel shows results at inverse temperature $\beta = 32$ in the whole region close to the $\rho = 1$ plateau. The middle ($n_{\max} = 2$) and bottom ($n_{\max} = 3$) panels show details around the left edge of the plateau at several inverse temperatures. The μ -value at which the large- β curves cross the line $\langle n \rangle = N - 1/2$ is used along with the analogous crossing with $\langle n \rangle = N + 1/2$ at the right end of the plateau to extract the Mott gap (i.e., the width of the $\langle n \rangle = N$ plateau).

compressibility can be written as

$$\kappa = \frac{1}{NT} \sum_{i=1}^{N_l} \left[\langle n_i^2 \rangle - \langle n_i \rangle^2 \right] \quad (5)$$

We will here consider the case where all the sizes N_i are finite, including also in the limit where the system size $N \rightarrow \infty$, to illustrate the large contributions from finite lakes in the standard scenario.

Figure 8 schematically illustrates the expected dependence of the average particle number of one of the lakes as a function of their total chemical potential (background value μ plus the random value ϵ_i). The plateaus shown corresponds to $\rho = 1$ (center) and one particle being added (right) or removed (left). If the half-width Λ of the disorder distribution exceeds half the Mott gap, $\Lambda > \Delta_M/2$, then the lake can have particle density different from the Mott background. We will estimate the contribution to the $T \rightarrow 0$ compressibility from all the

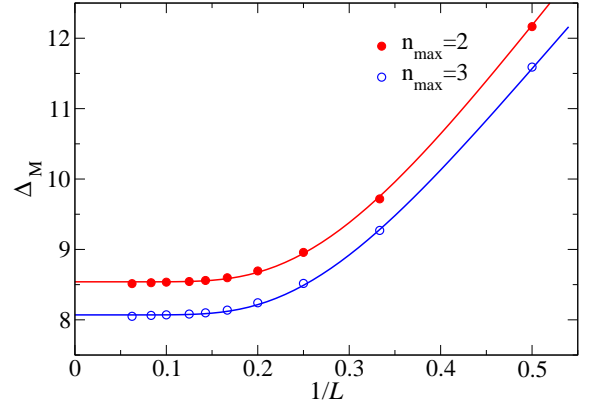


FIG. 7. (Color online) Determination of the Mott gap in the thermodynamic limit for the BHM with $\rho = 1$ at $U = 22$. The points are results of SSE simulations such as those shown in Fig. 6, with particle-number cut-offs equal to 2 and 3, and the curves are fits to the form $\Delta_M(L) = \Delta_M(\infty) + ae^{-bL}$, using system sizes $L \geq 5$. The results are $\Delta_M = 8.52(2)$ ($n_{\max} = 2$) and $\Delta_M = 8.10(2)$ ($n_{\max} = 3$).

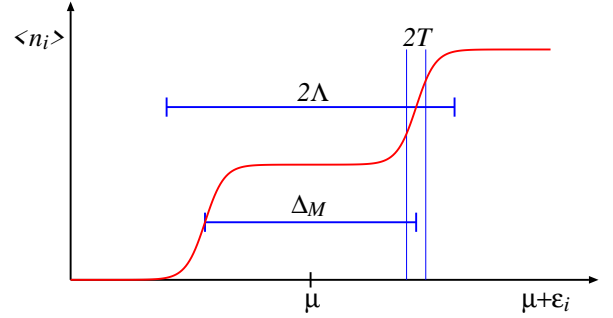


FIG. 8. (Color online) Particle number of a lake versus the total chemical potential $\mu + \epsilon_i$ of the lake. The width of the disorder distribution from which ϵ_i is drawn is 2Λ . Lakes for which $\mu + \epsilon_i$ falls within a distance roughly equal to the temperature from the value of μ at which the particle number jumps at $T = 0$ (this value being $\mu = \mu_0 + \Delta_M/2$, where μ_0 is the chemical potential at the center of the plateau) contribute to the $T \rightarrow 0$ compressibility.

lakes in this case. Note that this estimation only includes contributions from each lake coming from fluctuations by ± 1 particle. If Λ is sufficiently large higher fluctuations also contribute but do not change the overall picture we want to illustrate.

Roughly, as indicated in Fig. 8, there is a significant contribution from lake i if $\mu + \epsilon_i$ falls within a distance T (or a few times T) from the step at which the particle number of the lake changes. Within this window $\langle n_i^2 \rangle - \langle n_i \rangle^2$ is of order one, while outside the window this quantity is essentially zero. The probability of being inside the window is T/Λ , and, thus, on average a lake contributes of the order $1/(N\Lambda)$ to the total compressibility (5). Since the number of lakes $N_l \propto N$ we have the standard result that the compressibility of a system

of such lakes with random chemical potentials is non-zero and not very small as $T \rightarrow 0$. Clearly this would remain true also if the site energies are random within the lakes, in which case ϵ_i above should be the average chemical potential of a lake.

One crucial assumption made above was that Λ was larger than half of the Mott gap, so that particle-number sectors different from those corresponding to the Mott insulator can be reached. However, if the lakes are finite one should not here use the value of the Mott gap in the thermodynamic limit, but the finite-size Mott gap corresponding to the lake size (and also there will be shape effects). This size effect is likely at the heart of our finding that κ of the site-disordered BHM is very small in an extended region, not only very close to the MI-glass boundary but also well away from it. The finite-size Mott gap of course not only depends on the size of the lake but also on its shape. In the next section we will illustrate the effect of finite size using a few simple cluster shapes.

3. Single lake in a Mott background

Consider a lake A of arbitrary shape formed by a cluster of N_A sites with chemical potential $\mu_A = \mu + \epsilon_A$ embedded in a Mott insulating background B with chemical potential $\mu_B = \mu$ and periodic boundary conditions. The whole system has $N = L^2$ sites. The number of bosons in the system is n with n_A in A and n_B in B.

The compressibility of the whole system defined in (4) can be expressed as

$$\kappa = \frac{1}{NT} \left[\langle (n_A + n_B)^2 \rangle - \langle n_A + n_B \rangle^2 \right]. \quad (6)$$

Consider μ_A not far away from μ_B , so that the ground state of the whole system is in the Mott phase with n an integer multiple of N . The total compressibility at $T = 0$ vanishes. However, the number of bosons can still fluctuate in either subsystem by quantum tunneling through the boundaries. This example illustrates the fact that the basic assumption of the standard scenario and Eq. (5) are never strictly correct when $T \rightarrow 0$. The correlation between bosons in the lakes and in the background should be considered below some temperature which depends on the nature of the Mott background, the typical distance between the lakes, etc.

Now consider temperatures higher than these tunneling-dominated low temperatures. Then the thermal energy dominates, leading to mainly independent grand-canonical number fluctuations within the lakes. If μ_A is turned up large enough, we expect $n = n_A + n_B$ at low T to exhibit sharp (if T is not too high) steps, where the system becomes compressible. It is clear that the completely rigid Mott background assumption of the standard scenario, Eq. (5), must to some extent

fail at these compressible regions even at elevated temperatures. Strictly speaking it is the particle number n of the total system that jumps, though most of the excess or deficit particle number will be localized inside the region A of the modified chemical potential; the spread in excess density should be exponentially localized around region A. Thus, the boson number fluctuation inside lake A gives the essential contributions to the compressibility of the system when ϵ_A exceeds a certain value, which, according to the standard scenario, is half of the Mott gap. One can then apply the picture of independent lakes to the compressibility.

To elucidate the finite-size effects in this picture, we have carried out illustrative calculations for a single domain with modified (variable) chemical potential in a background of fixed chemical potential. We focus on the following question: At which μ_A does the embedded domain start to contribute to the compressibility? To answer this question we use SSE QMC calculations to study finite clusters embedded in a larger MI system. We set the chemical potential of the MI background to $\mu_B = 9.07$, which, as seen in Fig. 9, is at the center of the $\rho = 1$ Mott lobe of the clean BHM. As it is not possible to define an area surrounding the domain which would completely single out the compressibility contribution of the domain alone, we investigate the compressibility of the full system, i.e., the fluctuation of the total particle number $\langle n \rangle$. As discussed above, this should be essentially the same as the compressibility due to the embedded domain, given that the MI environment has a very substantial Mott gap and by itself has a very small compressibility.

a. Finite-size effect for an embedded square cluster

We consider a system with $U = 22$, studying first a square-shaped lake with linear size L_A embedded in a system with $L = 16$. Figures 9 and 10 show the density of bosons ρ and the compressibility κ as functions of μ_A of an $L_A = 2$ and an $L_A = 3$ lake, respectively. Here the inverse temperature is $\beta = 32$, which is low enough to resolve clearly the different particle-number sectors of relevance to our discussion here.

The compressibility κ is found to peak at values of μ_A corresponding to the steps in the density curves, where different particle-number sectors of the whole system are degenerate. The first peak on the right-hand side appears at $\mu_A(+)$ = 17.69 for $L_A = 2$ and at $\mu_A(+)$ = 16.07 for $L_A = 3$, respectively. These values correspond to the deviation in chemical potential,

$$\epsilon_A(+) = \mu_A(+) - \mu_B, \quad (7)$$

being much larger than $\Delta_M/2 \approx 4.3$. The first peak on the left-hand side appears at $\mu_A(-)$ = 1.69 for $L_A = 2$

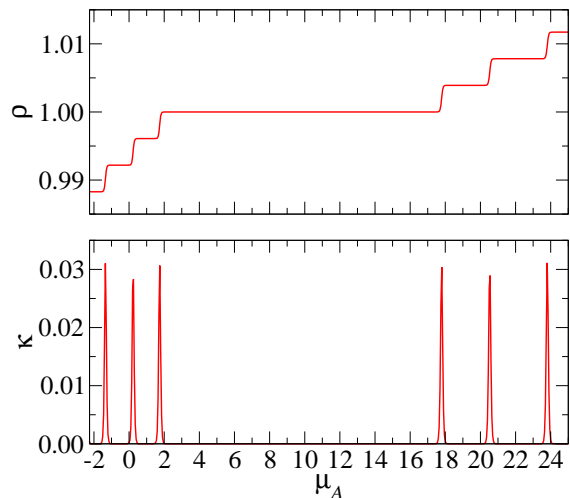


FIG. 9. (Color online) The particle density ρ (top panel) and the compressibility κ (bottom panel) of the $U = 22$ system with $L = 16$ at $\beta = 32$ as functions of the chemical potential μ_A .

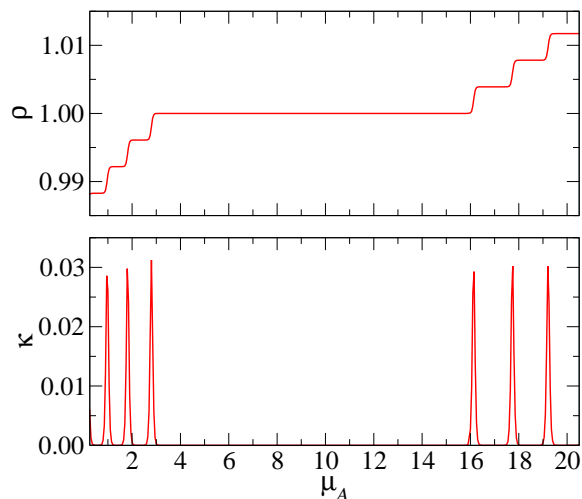


FIG. 10. (color online) The same quantities as in Fig. 9 but with a lake-size $L_A = 3$.

and at $\mu_A(-) = 2.77$ for $L_A = 3$, respectively. Again, they correspond to the deviation

$$\epsilon_A(-) = \mu_B - \mu_A(-) \quad (8)$$

being much larger than $\Delta_M/2$.

The value $\mu_A(+) - \mu_A(-)$ can be understood as an effective Mott gap of the finite embedded cluster, which is much larger than the Mott gap Δ_M . As the cluster size L_A increases, the gap shrinks and should approach Δ_M in the limit $L_A \rightarrow \infty$, as it appears to do roughly in the top panel of Fig. 11, where results are graphed for several L_A . There will of course be secondary finite-size

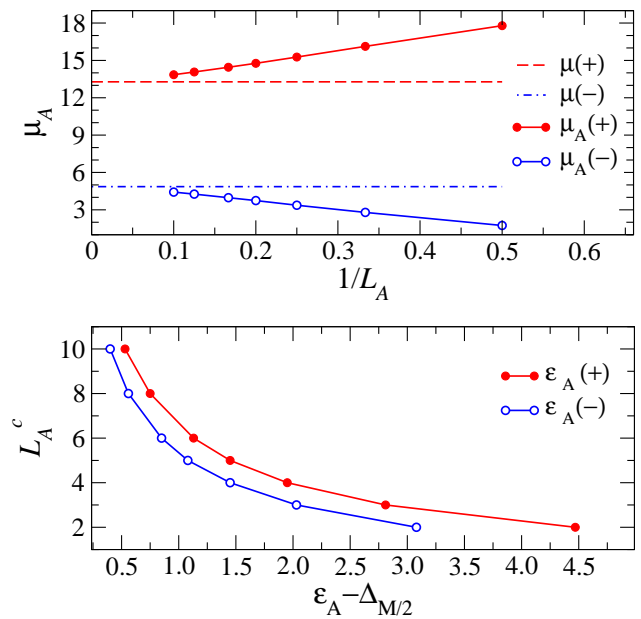


FIG. 11. (Color online) The top panel shows the finite-size Mott-gap boundaries $\mu_A(\pm)$ for a square cluster embedded in a Mott background as functions of the cluster size L_A . The boundaries are compared with the infinite-size Mott boundaries $\mu(+) - \mu(-) = \Delta_M$. The bottom panel shows the characteristic size L_A^c beyond which an embedded cluster system with chemical-potential shift ϵ_A leads to a compressible system.

effects here as well (i.e., beyond the dependence on L_A) when L_A approaches the full-system size L .

The above results imply that, given $\epsilon_A(\pm) > \Delta_M/2$ of a lake embedded in the MI, to contribute to the system's compressibility the cluster has to be larger than a characteristic size L_A^c . This size extracted from the data in the upper panel of Fig. 11 are graphed in the bottom panel of Fig. 11, for both added and removed particles. Clusters with size smaller than L_A^c are actually still Mott-like and should not be considered as superfluid lakes (though in general their properties can still be distinct from the Mott background, due to their altered spectral properties, which are related to their sizes and shapes). In the limit $\epsilon_A(\pm) \rightarrow \Delta_M/2$, the embedded cluster has to be infinitely large to contribute to the compressibility and this explains why the compressibility must still be exponentially decaying with temperature right at the MI-glass boundary, as we found in the main text.

b. Effect of cluster shape

The embedded clusters are in reality, in an actual site-disordered BHM, typically not of square shape. We now consider effects of cluster shape by comparing embedded clusters in the shape of a square, a cross, and a line. The number of sites in the clusters, embedded in the $L = 16$

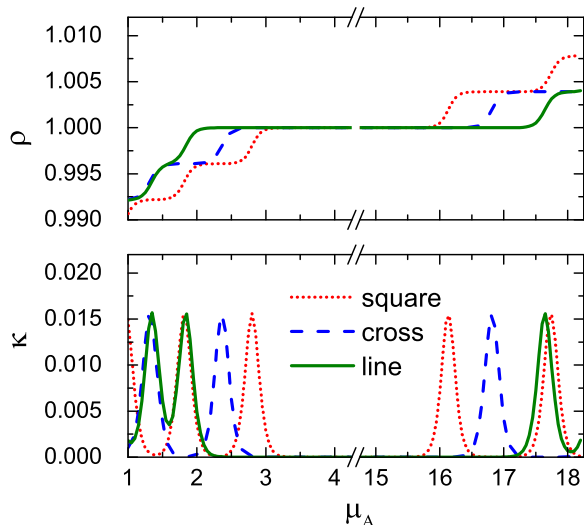


FIG. 12. (Color online). The density ρ (top panel) and compressibility κ (bottom panel) versus the chemical potential μ_A of the embedded clusters in the square, cross and line-shape, respectively. In all cases the cluster size is 9 sites and the inverse temperature $\beta = 16$.

Mott background, is $N_A = 9$ in all cases. The inverse temperature in the SSE simulations was $\beta = 16$, leading to significant temperature smoothing but still resolvable steps in the particle number, as shown in the top panel of Fig. 12. The line-shaped cluster and cross-shaped clusters have larger effective Mott gaps than that of the square cluster. This means that, for a given deviation $\epsilon_A(\pm) > \Delta_M/2$, the characteristic size required for non-zero compressibility of an irregularly shaped cluster is even larger than that of the squared one discussed in the previous section.

c. Conclusions

The main point argued here is that the Mott gap of “lake” embedded in the Mott background is enhanced by finite size (of the lake), and, as a direct consequence of this, the compressibility of the glass phase can be much smaller than would be expected based on the standard scenario of superfluid lakes (as most of the lakes will actually not contribute significantly). As discussed in the main text, effects of quantum-criticality with dynamic exponent $z \neq 2$ can further contribute to an anomalously small compressibility also close to the superfluid phase.

While we did not discuss in details effects of correlations in particle-number fluctuations between different lakes, these can also be expected to be ultimately important in the limit $T \rightarrow 0$. It would be interesting to carry out detailed studies of the effects of such correlations by considering two or more domains with altered chemical potential in a Mott background, generalizing the single-

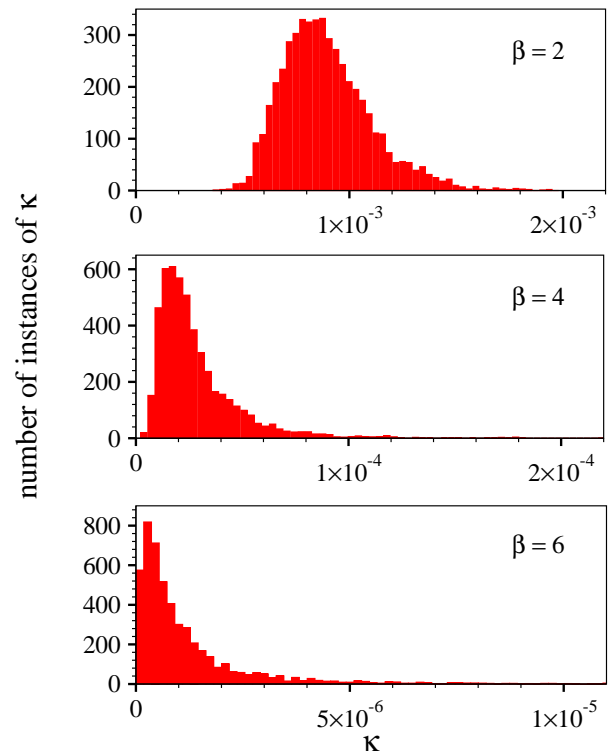


FIG. 13. (Color online). Histograms of the compressibility computed using approximately 5000 realization of random site potentials for an $L = 16$ lattice at $U = 22$, $\Lambda = 6$, and different values of the inverse temperature (as indicated in the panels)

lake calculations presented here.

4. Compressibility distribution

When considering disorder averages there is always a potential concern of long tails in the probability distributions of computed quantities, which may not be adequately samples with the relatively small number of disorder realizations used in typical QMC simulations. This issue may be particularly worrisome in a glass phase, where the low-energy fluctuations can be completely dominated by very rare configurations—in this case large lakes of superfluid in the MI background. If the anomalous glass phase we have demonstrated has a non-zero but very small compressibility in the limit $T \rightarrow 0$ [$c > 0$ in Eq. (2) in the main text], that very small compressibility should be exactly due to rare large superfluid lakes. Then the stretched exponential form we found for the T -dependent compressibility in the main text should exhibit a cross-over to a small essentially T -independent value below some temperature. We have not seen any signs of such cross-overs in the “finger” region in the phase diagram, but one may worry that the unexpectedly small compressibility and absence of a cross-over

could be due to poor sampling of rare disorder realizations with large compressibility. To investigate this issue, we have constructed histograms approximating the probability distribution $P(\kappa)$, examples of which are displayed in Fig. 13. While one may argue that very rare large- κ “events” are not sampled in practice, the probability distributions must have well-behaved functional forms, and one should be able to estimate effects of large- κ regions not sampled by investigating the tail-parts of the distributions that actually are sampled in simulations with a typical number (here thousands) of random samples.

It is clear, as seen in Fig. 13, that the distribution becomes increasingly skewed as the temperature is lowered, with a thin high- κ tail developing. The whole distribution moves rapidly toward lower values, however, and the tail is not sufficiently long or fat to cause serious problems with properly converging the mean compressibility. The results are consistent with an exponentially decaying tail and all indications are that we have collected an adequate number of configurations for correctly estimating the disorder-average of the compressibility at all temperatures studied. We can of course still not rule out more significant tails at lower temperatures than we have studied here. Relatively longer and more prominent tails in fact appear likely based on our results, but do not by themselves necessarily imply a non-zero $\kappa(T \rightarrow 0)$.

5. Effects of the particle-number cut-off

In the SSE method we have used,[30] it is necessary to impose a cut-off on the site-occupation numbers, $n_i \leq n_{\max}$. This can be seen as an approximation, or it can simply be regarded as modifying the BHM with an effective U which depends on the occupation number, i.e., $U(n_i) = \infty$ for $n_i > n_{\max}$. This is a perfectly reasonable model with the same symmetries as the original BHM. In practice, the BHM with large U “self-imposes” a cut-off, in the sense that the probability of occupying a site with many particles becomes exceedingly small. In the SSE method one can also use a high enough cut-off for there to be no detectable effects of the cut-off at all. However, since we are studying disordered systems and have to carry out averages over (typically) thousands of realizations of the random potentials, it is useful to have a small cut-off because that speeds up the calculations. The salient properties of these two versions of the model should not be expected to differ much in the parameter regions we have studied.

Nevertheless, to check for effects of the cut-off, in addition to the main results obtained with $n_i \leq 2$, we have also carried out some calculations with $n_i \leq 3$ and $n_i \leq 4$. We have already discussed the small effects of restricting the on-site occupation numbers to $n_i \leq n_{\max}$ in Sec. 1. Here we discuss effects on the compressibility.

Fig. 14 shows the $\Lambda = 6$ data from Fig. 3 in the main

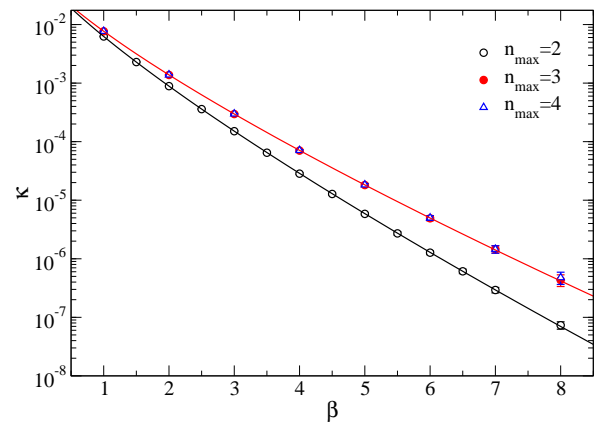


FIG. 14. (Color online) The compressibility at $U = 22$, $\Lambda = 6$ computed with different cut-offs n_{\max} in SSE simulations of $L = 16$ systems. The curves are fits to the stretched exponential form, Eq. (9), using $\beta = 4$ and higher in the fits (but also the behavior at lower β is seen to match well the resulting fits). The parameters are $b \approx 2.85$, $\alpha \approx 0.78$ for $n_{\max} = 2$ and $b \approx 2.66$, $\alpha \approx 0.75$ for $n_{\max} = 3$ (and there are no statistically significant differences between $n_{\max} = 3$ and 4).

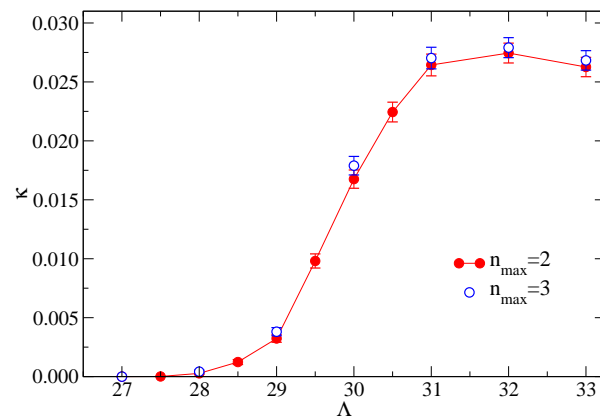


FIG. 15. (Color online) Compressibility versus disorder strength for $L = 8$ systems at $U = 60$ and inverse temperature $\beta = 8$, calculated with cut-offs $n_{\max} = 2$ and 3.

text, which was computed with $n_{\max} = 2$, along with data also for $n_{\max} = 3$ and 4. While, as would be expected, a higher cut-off enhances the compressibility, the stretched exponential form proposed in the main text,

$$\kappa \propto e^{-b/T^\alpha} \quad (9)$$

is robust. Interestingly, the exponent α only changes from $\alpha \approx 0.78$ for $n_{\max} = 2$ to $\alpha \approx 0.75$ for $n_{\max} = 3$, while the effect on the prefactor b multiplying $T^{-\alpha}$ in the exponential is somewhat larger (values given in the caption of Fig. 14). Within the temperature range studied, there are no detectable differences between the results for $n_{\max} = 3$ and $n_{\max} = 4$.

Fig. 15 shows the compressibility in the parameter region of the inset of Fig. 2 in the main paper, but us-

ing $L = 8$ instead of $L = 16$ and comparing results for $n_{\max} = 2$ and 3. There are no significant differences between the two data sets (perhaps just a small enhancement of κ when $n_{\max} = 3$). In addition to confirming the negligible effects of the cut-off $n_{\max} = 2$, these results also demonstrate the small size effects in this region (as the results agree very closely with those for $L = 16$ in the main paper). The small effects of the cut-off in this region is perhaps not surprising considering that the repulsion $(U/2)n(n-1) = 180$ for $n = 3$, making triple and quadruple occupancy of the sites very small even on sites with the smallest site energies even when $\Lambda \approx 30$.

In conclusion, the restriction $n_i \leq n_{\max} = 2$ considered in the main paper some times has small quantitative effects on the results (relative to having no cut-off at all), but qualitatively the properties of the model are the same, e.g., a stretched exponential form of the temperature dependent compressibility in the state we have termed the anomalous Bose-glass, and the existence of a sharp cross-over (perhaps turning into a phase transition in some parts of the phase diagram) between this almost incompressible state and a normal highly compressible Bose-glass. One would also not expect universal physics of the model to depend on the cut-off (e.g., the dynamic exponent z determined in the main text), as no symmetries are changed and the cut-off also can be considered as a minor modification of the on-site repulsion.

* e-mail: waguo@bnu.edu.cn

† e-mail: sandvik@bu.edu

- [1] T. Giamarchi and H. J. Schulz, Phys. Rev. B **37**, 325 (1988).
- [2] M. P. A. Fisher, P. B. Weichman, G. Grinstein, and D. S. Fisher, Phys. Rev. B **40**, 546 (1989).
- [3] J. K. Freericks and H. Monien, Phys. Rev. B **53**, 2691 (1996).
- [4] G. G. Batrouni, V. Rousseau, R. T. Scalettar, M. Rigol, A. Muramatsu, P. J. H. Denteneer, and M. Troyer, Phys. Rev. Lett. **89**, 117203 (2002).
- [5] B. Capogrosso-Sansone, S. G. Söyler, N. Prokofev, and B. Svistunov, Phys. Rev. A **77**, 015602 (2008).
- [6] K. W. Mahmud, E. N. Duchon, Y. Kato, N. Kawashima, R. T. Scalettar, and N. Trivedi, Phys. Rev. B **84**, 054302 (2011).
- [7] M. Greiner, O. Mandel, T. Esslinger, T. W. Hänsch, and I. Bloch, Nature **415**, 39 (2002).
- [8] I. Bloch, J. Dalibard, and W. Zwerger, Rev. Mod. Phys. **80**, 885 (2008).
- [9] B. Damski, J. Zakrzewski, L. Santos, P. Zoller, and M. Lewenstein, Phys. Rev. Lett. **91**, 080403 (2003).
- [10] L. Fallani, J. E. Lye, V. Guarrera, C. Fort, and M. Inguscio, Phys. Rev. Lett. **98**, 130404 (2007).
- [11] W. Krauth, N. Trivedi, and D. Ceperley, Phys. Rev. Lett. **67**, 2307 (1991).
- [12] M. Wallin, E. S. Sørensen, S. M. Girvin, and A. P. Young, Phys. Rev. B **49**, 12115 (1994).
- [13] T. Giamarchi, P. Le Doussal, and E. Orignac, Phys. Rev. B **64**, 245119 (2001).
- [14] J.-W. Lee, M.-C. Cha, and D. Kim, Phys. Rev. Lett. **87**, 247006 (2001).
- [15] F. Pázmándi and G. T. Zimányi, Phys. Rev. B **57**, 5044 (1998).
- [16] J. Wu and P. Phillips, Phys. Rev. B **78**, 014515 (2008).
- [17] F. Alet and E.S. Sørensen, Phys. Rev. E **67**, 015701 (2003).
- [18] N. V. Prokof'ev and B. V. Svistunov, Phys. Rev. Lett. **92**, 015703 (2004).
- [19] P. Sengupta and S. Haas, Phys. Rev. Lett. **99**, 050403 (2007).
- [20] P. B. Weichman and R. Mukhopadhyay, Phys. Rev. B **77**, 214516 (2008).
- [21] L. Pollet, N. V. Prokof'ev, B. V. Svistunov, and M. Troyer, Phys. Rev. Lett. **103**, 140402 (2009).
- [22] V. Gurarie, L. Pollet, N. V. Prokof'ev, B. V. Svistunov, and M. Troyer, Phys. Rev. B **80**, 214519 (2009).
- [23] F. Krüger, S. Hong, and P. Phillips, Phys. Rev. B **84**, 115118 (2011).
- [24] F. Lin, E. S. Sørensen, and D. M. Ceperley, Phys. Rev. B **84**, 094507 (2011).
- [25] S. G. Söyler, M. Kiselev, N. V. Prokofev, and B. V. Svistunov, Phys. Rev. Lett. **107**, 185301 (2011).
- [26] E. Altman, Y. Kafri, A. Polkovnikov, and G. Refael, Phys. Rev. Lett. **93**, 150402 (2004).
- [27] E. Altman, Y. Kafri, A. Polkovnikov, and G. Refael, Phys. Rev. B **81**, 174528 (2010).
- [28] S. Iyer, D. Pekker, and G. Refael, Phys. Rev. B **85**, 094202 (2012).
- [29] T. Roscilde and S. Haas, Phys. Rev. Lett. **99**, 047205 (2007).
- [30] O. F. Syljuåsen and A. W. Sandvik, Phys. Rev. E **66**, 046701 (2002); O. F. Syljuåsen, Phys. Rev. E **67**, 046701 (2003).
- [31] R. B. Griffiths, Phys. Rev. Lett. **23**, 17 (1969).
- [32] B. M. McCoy, Phys. Rev. Lett. **23**, 383 (1969).
- [33] T. Vojta, J. Phys. A, Math. Gen. **39**, R143 (2006).
- [34] A percolation scenario for the transition into the SF state has recently been argued within mean-field calculations in which SF sites forming clusters were identified; A. Niederle and H. Rieger, New J. Phys. **15**, 075029 (2013). Percolation of the clusters signal the glass-SF transition and the phase boundaries obtained in this way agree astonishingly well with previous QMC calculations.
- [35] N. Ma, A. W. Sandvik, and D.-X. Yao, Phys. Rev. B **90**, 104425 (2014).
- [36] D. Stauffer and A. Aharony, *Introduction to Percolation Theory* (Taylor & Francis, Philadelphia, 1994).
- [37] H. Meier and M. Wallin, Phys. Rev. Lett. **108**, 055701 (2012).
- [38] A. Priyadarshree, S. Chandrasekharan, J.-W. Lee, and H. U. Baranger, Phys. Rev. Lett. **97**, 115703 (2006).
- [39] Here we use the compressibility at the smallest non-zero wave-number, $\kappa(q = 2\pi/L)$, which has smaller relative statistical errors than $\kappa(q = 0)$. The two quantities have the same scaling properties; L. Wang, K. S. D. Beach, and A. W. Sandvik, Phys. Rev. B **73**, 014431 (2006).
- [40] M. Hohenadler, M. Aichhorn, S. Schmidt, L. Pollet, Phys. Rev. A **84**, 041608(R) (2011).